Ecotoxicology and Environmental Safety 222 (2021) 112553

Contents lists available at ScienceDirect

Ecotoxicology and Environmental Safety

journal homepage: www.elsevier.com/locate/ecoenv

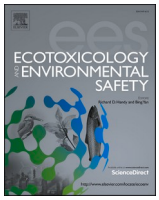

Specific toxicity of azithromycin to the freshwater microalga *Raphidocelis subcapitata*

Ana Catarina Almeida *, Tânia Gomes, Jose Antonio Baz Lomba, Adam Lillicrap

Norwegian Institute for Water Research (NIVA), Gaustadalléen 21, Oslo 0349, Norway

ARTICLE INFO

Edited by: Paul Sibley

Keywords:
Raphidocelis subcapitata
Antibiotic
Azithromycin
Flow cytometry
PAM fluorometry
Ecotoxicological effects

ABSTRACT

Pharmaceuticals are produced to inflict a specific physiological response in organisms. However, as only partially metabolized after administration, these types of compounds can also originate harmful side effects to non-target organisms. Additionally, there is still a lack of knowledge on the toxicological effects of legacy pharmaceuticals such as the antibiotic azithromycin. This macrolide occurs at high concentrations in the aquatic environment and can constitute a threat to aquatic organisms that are at the basis of the aquatic food chain, namely microalgae. This study established a high-throughput methodology to study the toxicity of azithromycin to the freshwater microalga *Raphidocelis subcapitata*. Flow cytometry and pulse amplitude modulated (PAM) fluorometry were used as screening tools. General toxicity was shown by effects in growth rate, cell size, cell complexity, cell viability and cell cycle. More specific outcomes were indicated by the analysis of mitochondrial and cytoplasmatic membrane potentials, DNA content, formation of ROS and LPO, natural pigments content and photosystem II performance. The specific mode of action (MoA) of azithromycin to crucial components of microalgae cells was revealed. Azithromycin had a negative impact on the regulation of energy dissipation at the PSII centers, along with an insufficient protection by the regulatory mechanisms leading to photodamage. The blockage of photosynthetic electrons led to ROS formation and consequent oxidative damage, affecting membranes and DNA. Overall, the used methodology exhibited its high potential for detecting the toxic MoA of compounds in microalgae and should be considered for future risk assessment of pharmaceuticals.

1. Introduction

The presence of antibiotics in the aquatic environment has been a growing concern. These are biologically active molecules intended to originate a physiological response in organisms. Following administration, antibiotics can undergo an incomplete metabolization, with a large amount being expelled unchanged or as biologically active metabolites ending in the aquatic environment (EEA, 2010; Kemper, 2008). Furthermore, there is still insufficient ecotoxicological data on several antibiotics (Välitalo et al., 2017), such as for azithromycin that has been quantified at relatively high values in the aquatic environment. In a study analysing the concentration of 17 antibiotics in different Wastewater Treatment Plants (WWTPs) from Portugal, Spain, Cyprus, Ireland, Germany, Finland and Norway, concentrations between 45.2 ng/L (Cyprus) and 597.5 ng/L (Portugal) were observed (Rodriguez-Mozaz et al., 2020). Maximum concentrations of 1.6 μg/L and 1.22 μg/L have also been detected in effluents in Portugal (Rodriguez-Mozaz et al., 2020) and in Slovakia (Birošová et al., 2014), respectively. Therefore, this antibiotic can be considered of high ecotoxicological relevance as it is not only widely applied and frequently detected in the aquatic environment, but also considered persistent and toxic at low concentrations, therefore posing a risk to the aquatic environment (Rodriguez-Mozaz et al., 2020; Välitalo et al., 2017).

Although antibiotics are intended to specifically target diseases caused by microorganisms such as bacteria, several studies have shown that they can also inflict damage to non-target organisms, as for instance microalgae (Aristilde et al., 2010; Ebert et al., 2011; Liu et al., 2011a; Pinckney et al., 2013). Their presence in the aquatic environment can therefore threaten microalgae that are vital to ecosystem function (Martinez et al., 2015). However, little is known on the specific harmful effects that these compounds can impose on microalgae species.

Most of the toxicity bioassays using microalgae only apply integrative endpoints such as the well-known algal growth inhibition test. Although ecologically relevant, this endpoint only indicates the general toxicity of a contaminant. Normally less sensitive and not useful to detect sublethal effects, this test does not provide any indication on how

* Correspondence to: Norwegian Institute for Water Research (NIVA), Section of Ecotoxicology and Risk Assessment, Gaustadalléen 21, N-0349 Oslo, Norway.
E-mail address: ana.catarina.almeida@niva.no (A.C. Almeida).

https://doi.org/10.1016/j.ecoenv.2021.112553
Received 12 April 2021; Received in revised form 12 July 2021; Accepted 21 July 2021
Available online 26 July 2021

a contaminant disrupt the biological processes in microalgal cells - its toxic mode of action (MoA). Currently, more specific endpoints are being used which can offer initial warning signs on the possible detrimental effects of antibiotics to microalgae (Adler et al., 2007; Esperanza et al., 2015; González-Pleiter et al., 2017; Prado et al., 2009).

Flow cytometry (FCM) is a diagnostic tool that can be applied to analyse the metabolic status of microalgal cells. It allows fast acquisition of data with several fluorometric and light-scatter parameters being analysed in individual cells. This method has already been used to identify the effects of different classes of compounds on several microalgae species (Franklin et al., 2001; Franqueira et al., 2000; Míguez et al., 2021; Seoane et al., 2014; Stauber et al., 2002). The collected data allows extrapolation from specific results on an organism to those at the population level, which can be beneficial for environmental risk assessment. Parameters such as cell size and complexity and natural pigment content in microalgal cells can be analysed by their autofluorescence (Adler et al., 2007; Franklin et al., 2001). Additionally, fluorescent probes can also be used to detect alterations in different metabolic mechanisms. Unique probes exist to differentiate biochemical processes such as caspase activity (Esperanza et al., 2017), intracellular pH and free calcium (Prado et al., 2012a), the formation of reactive oxygen species (ROS) and lipid peroxidation (LPO), cytoplasmatic and mitochondrial membrane potential, cell viability and metabolic activity, as well as cell cycle and DNA content (Almeida et al., 2019).

The fluorescence of chlorophyll *a* is another responsive endpoint to analyse the toxicity of contaminants to microalgae (Juneau and Popovic, 1999; Ralph et al., 2007). This procedure relies on chlorophyll fluorescence imaging of microalgae samples in microplates using an imaging PAM fluorometer. This permits a fast and precise measurement of phytotoxicity, with simultaneous measurements of many samples (Schreiber et al., 2007). This technique has already been applied on analysing the toxicity of metals, herbicides, gamma radiation and nanoplastics towards microalgae (Almeida et al., 2019, 2017; Gomes et al., 2020).

The present study intended to determine the specific toxic effects of azithromycin to the freshwater microalgae *Raphidocelis subcapitata*. This algal species is a recommended ecotoxicological bioassay by the Organization for Economic Cooperation and Development (OECD, 2011), as it is generally more sensitive than other microalgal species (Rojíčková and Maršálek, 1999). *R. subcapitata* is frequently detected in freshwater and is easy to culture in laboratory conditions, with a brief generation period and high growth rate (OECD, 2011; Suzuki et al., 2018). In the present study, algae were exposed to azithromycin and several endpoints were investigated including growth rate, natural pigments content, PSII performance, cell size, cell complexity, cell viability, cell cycle and DNA content, formation of ROS (chloroplasts and mitochondria), mitochondrial and cytoplasmatic membrane potentials and LPO.

2. Material and methods

2.1. Microalga cultures

Experiments were made using the unicellular freshwater microalgae *R. subcapitata* (NIVA-CHL 1, Norwegian Institute for Water Research, Oslo, Norway). Cultures were kept in 50 mL glass flasks with an initial number of 10×10^3 cells/mL in ISO 8692 medium (ISO, 2012), prepared at least 24 h before use. Cultures were in an exponential growth phase, incubated for 3–4 days in an incubator (Innova 1, 44 R, incubator shaker series, New Brunswick Scientific, Eppendorf AG, Germany) at 22 ± 2 °C, with orbital shaking at 90 rpm and under continuous illumination from day light-type fluorescent tubes (60.61–61.48 μmol.s^{-1}.m^{-2}).

2.2. Algal exposure

Experiments were performed at identical conditions as those previously described for the cultures (22 ± 2 °C, orbital shaking at 90 rpm and under continuous illumination in an incubator), and at an initial cell concentration of 10×10^3 cells/mL. Exponentially growing microalgae were exposed to azithromycin in batch cultures over 72 h. Media as specified in 8692:2012 (ISO, 2012) was used for the controls. Preliminary studies were made to analyse the general toxicity of azithromycin to *R. subcapitata*, using the 72 h algal growth inhibition test, according to the ISO guideline (ISO, 2012). The effect concentrations EC_{10}, EC_{20} and EC_{50} were calculated (data is shown in Table A1 and Fig. A1 in Supporting Information, SI) to select which concentrations to use for the subsequent studies, to determine specific sub-lethal effects of azithromycin to *R. subcapitata*. Experiments were performed at least twice in 25 mL glass flasks with 15 mL of test volume, with six replicates for the control and triplicates for the exposed samples. After the 72 h exposure, algal samples were collected for further analyses of specific toxic endpoints. The remaining volume was used for chemical analysis.

2.3. Test compound and chemical analysis

The test compound azithromycin dihydrate (CAS number: 117772–70–0; article number PZ0007) was purchased from Sigma-Aldrich (United Kingdom) with ≥98.0% purity. Sample extraction for chemical analysis was made using Waters Oasis HLB μElution plates, 30 μm (Milford, MA, USA). The plate was washed and rinsed with 1 mL of methanol (MeOH) and 1 mL of ultrapure water under suction. Samples collected at the beginning (0 h) and end (72 h) of algal exposures were provided in glassware and were homogenized before extraction. Subsequently, 1 mL of sample was loaded onto the plate under suction and the plate vacuum dried for 15 min. Azithromycin was eluted into a 96 well plate using 200 μL of MeOH. Final eluates were transferred into LC vials with the addition of 300 μL of ultrapure water prior to vortexing before analysis. Quantification was performed using an addition curve in duplicate by spiking known concentrations of azithromycin in the same matrix used for the study. The addition curve was prepared with the following concentrations: 0.2, 0.5, 1, 2, 5, 10, 20, 50 and 100 μg/L. The limits of quantification of the analytical method were calculated in those samples as the concentrations giving a signal-to-noise ratio (S/N) of ≥ 10.

Analysis was performed in a Waters Acquity UPLC system (Milford, MA, USA) equipped with a binary solvent manager and a sample manager. The UPLC was coupled to a Waters Xevo TQ-S triple quadrupole mass spectrometer (Milford, MA, USA) with electrospray ionization interface (ESI), operated in positive ionization mode. Selected parent and product ions together were 749.30 > 591.30 and 749.30 > 83.00, cone voltage of 30 V for both and collision energies of 30 and 50 V, respectively. Chromatographic separation was made using a Waters Acquity UPLC CORTECST C18 + 1.6 μm (Milford, MA, USA). The column temperature was kept at 45 °C and the temperature of the sample manager was 4 °C. A constant flow rate of 0.4 mL min^{-1} was used with a mobile phase consisting of 0.05% formic acid and 5 mM ammonium acetate in ultra-pure water (solvent A) and acetonitrile:methanol 3:1 (solvent B). The elution gradient changed as follows: 0 min (0% B); 1.5 min (0% B); 2.5 min (90% B); 5 min (90% B); 5.5 min (0% B) and 6.5 min (0% B). The sample injection volume was 3 μL and the retention time for azithromycin was 2.9 min.

2.3.1. FCM analysis

An Accuri™C6 Flow Cytometer (BD Biosciences, San Jose, USA) with argon-ion excitation lasers (488 nm and 640 nm) was used for the FCM analysis. All endpoints were acquired in microalgae cells exposed for 72 h to different concentrations of azithromycin, besides absolute cell counts that were also analysed after 24 h and 48 h. A threshold set on FSC-H was used. Algal cells were gated using the chlorophyll autofluorescence of control cells by displaying FL3-A (laser exicator 488 nm, filter >670 nm) *versus* FL4-A (laser exicator 640 nm, filter 6705/25 nm (Almeida et al., 2019). 10,000 cells were collected per sample, gated and analysed using the BD AccuriTM C6 software version 1.0.264.21. The

mean fluorescence value was used for each sample and final data was expressed as fold induction compared to control (mean ± SEM; a.u. – arbitrary units). Representative dot-plots and histograms used to characterize microalgae cells are in Fig. A2 on the SI. For all the assayed probes, the 488 nm argon-ion laser was used. Number of cells, concentration of probes and incubation conditions were all previously optimized and based on previous studies (Almeida et al., 2019).

2.3.1.1. Cell counting, cell size, complexity and natural pigments content. Algal growth was calculated using the absolute cell counting as a function of time, recorded at 24 h, 48 h and 72 h, and compared with the control (*R. subcapitata* in ISO 8692 media). The procedure was based on the guidelines OECD 201 (OECD, 2011) and ISO 8692:2012 (ISO, 2012). The specific growth rate (μ, d^{-1}) was calculated from the initial cell concentration and those at each time point (24 h, 48 h and 72 h) by the equation:

$$\mu_{n-0} = \frac{\ln \quad (N_n) - \ln(N_0)}{t_n - t_0} \times 24 \quad \left(day^{-1}\right)$$

μ_{n-0} is the average specific growth rate from time 0 to n, N_n is the cell density at time n and N_0 is the cell density at time 0. The growth rate was indicated as fold induction compared to control. The effective concentrations EC_{10} (effective concentration for 10% reduction), EC_{20} (effective concentration for 20% reduction) and EC_{50} (effective concentration for 50% reduction), NOEC (the no observed effect concentration) and LOEC (lowest observed effect concentration) were calculated for each time point.

Cell size was set by displaying cell counts *versus* FSC-A (forward scatter), while cell complexity by counts *versus* SSC-A (side scatter). The content of chlorophyll *a* and *b*, carotenoids, xanthophyll and peridinin, used to indicate the content of the natural pigments, were quantified by using the natural autofluorescence of algal cells (Table A2 in SI).

2.3.1.2. Cell viability and metabolic activity. Cell viability and metabolic activity were determined by the inhibition of fluorescein diacetate (FDA; Invitrogen, ThermoFisher Scientific, Eugene, OR, USA), according to (Almeida et al., 2019). The cell viability index was calculated as:

$$\frac{(FDA \quad fluorescence \quad mean) \times (number \quad of \quad stained \quad events)}{(Green \quad autofluorescence \quad mean) \times (number \quad of \quad events)}$$

The percentage of viable and non-viable cells (Gala and Giesy, 1990) was also calculated according to (Almeida et al., 2019).

2.3.1.3. ROS formation. ROS formation was measured using two probes, carboxy-H_2DFFDA (carboxy-2′,7′-difluorodihydrofluorescein diacetate, Invitrogen, ThermoFisher Scientific, Eugene, OR, USA) and DHR 123 (dihydrorhodamine 123; Invitrogen, ThermoFisher Scientific, Eugene, OR, USA), as previously described in (Almeida et al., 2019, 2017) and (Gomes et al., 2020).

2.3.1.4. Cytoplasmatic and mitochondrial membrane potential. To measure cytoplasmatic membrane potential (CMP), the fluorescence probe $DiBAC_4(3)$ (bis-(1,3-dibutylbarbituric acid) trimethine oxonol; Invitrogen, ThermoFisher Scientific, Eugene, OR, USA) was used. A working solution with 0.97 μM as final concentration in 1 mL of sample was set for staining (Prado et al., 2012b). After thirty minutes incubation at room temperature and in the dark, the fluorescence was analysed in the FL1 channel (488 nm excitation, 533/30 emission).

The mitochondrial membrane potential (MMP) was quantified using the fluorescence probe $DiOC_6(3)$ (3,3'-dihexyloxacarbocyanine iodide; Invitrogen, ThermoFisher Scientific, Eugene, OR, USA). For staining, a working solution (final concentration of 30 nM) was set by diluting the probe in 1 mL of exposed microalgae (Grégori et al., 2003). Incubation was thirty minutes at room temperature in the dark. Probe fluorescence was analysed in the FL1 channel (488 nm excitation, 533/30 emission).

2.3.1.5. Lipid peroxidation (LPO). The lipophilic fluorescent probe C_{11}-$BODIPY^{581/591}$ (4,4-difluoro-5-(4-phenyl-1,3-butadienyl)−4-bora-3a,4a-diaza-s-indacene-3-undecanoic acid; Invitrogen, ThermoFisher Scientific, Eugene, OR, USA) was used to determine the oxyl-radical induced lipid oxidation (LPO), as described in (Almeida et al., 2019, 2017).

2.3.1.6. DNA content e cell cycle. DNA content was analysed using PicoGreen (Invitrogen, ThermoFisher Scientific, Eugene, OR, USA), according to (Almeida et al., 2019).

The three cell cycle stages G1, S, and G2 were set using histograms of cell number *versus* fluorescence (Almeida et al., 2019; Marie et al., 1996; Veldhuis et al., 2001). Illustrative histograms for *R. subcapitata* unexposed and exposed cells are in Fig. A3 on the SI. DNA content in the different phases was calculated as:

$$\frac{(Picogreen \quad mean \quad fluorescence \quad)}{\%\quad of \quad plot}$$

The % of plot is the % of the different phases of the cell cycle.

2.3.2. Photosystem II (PSII) performance

Chlorophyll *a* fluorometry was used to determine PSII performance in microalgae exposed to azithromycin, following the method in (Almeida et al., 2019). After the 72 h exposure, *R. subcapitata* cells were up concentrated by centrifugation at 4200 rpm for 15 min at room temperature, after which the resulting pellet was resuspended in ISO media. 200 μl of each replicate sample were moved in duplicate to a 96-well black microplate (Corning Incorporated, Costar®, NY, USA) and dark acclimated for 30 min to let complete oxidation of PSII reaction centers. Following this, chlorophyll *a* fluorescence was measured using a pulse amplitude modulated (PAM) fluorometer (IMAGING-PAM, Heinz Walz GmbH, Effeltrich, Germany) with ImagingWin software (Heinz Walz GmbH PAM, Effeltrich, Germany). After the acquisition of the minimum and maximum fluorescent yields of PSII (F_0 and F_m, respectively), cells previously acclimated to dark were illuminated by an actinic light at an intensity equal to incubation light (~80 $\mu mol.m^{-2}.s^{-1}$) and the current fluorescence yield (F_t), the minimum fluorescence yield in the light ($F_{0'}$) and the maximum fluorescence yield in the light ($F_{m'}$) values recorded. Thirteen parameters of interest, the maximal PS II quantum yield (F_v/F_m), the efficiency of the oxygen-evolving complex (OEC), the effective PS II quantum yield (Y(II)), the quantum yield of regulated energy dissipation (Y(NPQ)), the quantum yield of nonregulated energy dissipation (Y(NO)), the coefficients of photochemical quenching (qP and qL), the coefficient of non-photochemical quenching (qN), the non-photochemical quenching (NPQ), the relative photosynthetic electron transport rate (ETR), the relative photochemical quenching ($qP_{(rel)}$), the relative non-photochemical quenching ($qN_{(rel)}$) and the relative unquenched fluorescence ($UQF_{(rel)}$) were quantified according to the formulas depicted in Table A3 (SI).

2.4. Statistical analysis

Data from two independent experiments were pooled together, expressed as fold induction and presented as mean ± standard error of mean (SEM). The statistical program ToxRatPro© (version 3.3.0) was used to calculate the growth rate, EC_{10}, EC_{20}, EC_{50}, NOEC and LOEC. The XLStat2020® software (Addinsoft, Paris, France) was used for all the other statistical analyses and GraphPad Prism 8 software (GraphPad Software Inc., La Jolla, CA, USA) for graphical representations. For normally distributed data and with homogeneous variance, the parametric tests one-way ANOVA with Tukey post hoc were used for multiple comparisons. Non-normally distributed data and/or with non-homogeneous variance, the non-parametric Kruskal-Wallis and Dunn's post hoc tests were used. A non-linear regression using a sigmoidal dose-response curve with variable slope (four parameters) was applied for the

growth rate analysis according to:

$$f(x) = y\min + \frac{y\max - \ y \ \ min}{1 + 10^{((Log \ \ EC_{50} - x) \times Hill \ \ Slope)}}$$

being f the effect, x the concentration of the compound, y min the bottom (variable), y max the top (variable) and EC_{50} the concentration of the compound with an effect of 50% when normalized to the top and bottom values.

A Principal Component Analysis (PCA) was applied to distinguish the principal variables accountable for data variance. A Pearson correlation analysis was also used to indicate the association between variables. A p value < 0.05 was applied.

3. Results

3.1. Chemical analysis

The chemical analysis for azithromycin in the different samples collected at 0 h and 72 h of exposure are presented in Table A4 in SI. Results for all tested concentrations at the start of exposure were accurate compared to the nominal concentrations. Consequently, as the measured concentrations did not surpass ± 20% difference from nominal concentrations, the nominal concentrations were used. Two control samples (no azithromycin) were also analysed in parallel for quality control, for which no azithromycin levels were detected. Extraction blanks using the HLB extraction procedure also had negative identification, thus rejecting any possibility of cross-contamination. The stock solution of azithromycin (10 μg/mL) used to perform the test concentrations was also analysed after dilution, for which a nearly identical concentration of 10.28 μg/mL (n = 5) was determined.

To further analyse the stability of the compound over time, an extra analysis was performed at the end of exposure (72 h). Data indicated that azithromycin concentrations decreased approximately 30% during the exposure period (Table A4 in SI).

3.2. Microalgal toxicity bioassays

3.2.1. Growth rate, cell viability, metabolic activity and cytoplasmatic membrane potential (CMP)

The three concentrations selected to study the specific sub-lethal effects of azithromycin, were lower than the EC_{20} (0.026 mg/L after 72 h; Table A1 in SI): 0.002 mg/L, 0.006 mg/L and 0.02 mg/L. The growth rate (d^{-1}) curves for the 24 h, 48 h and 72 h exposure are shown in Fig. A1 in the SI, along with the EC_{10}, EC_{20}, EC_{50}, NOEC and LOEC

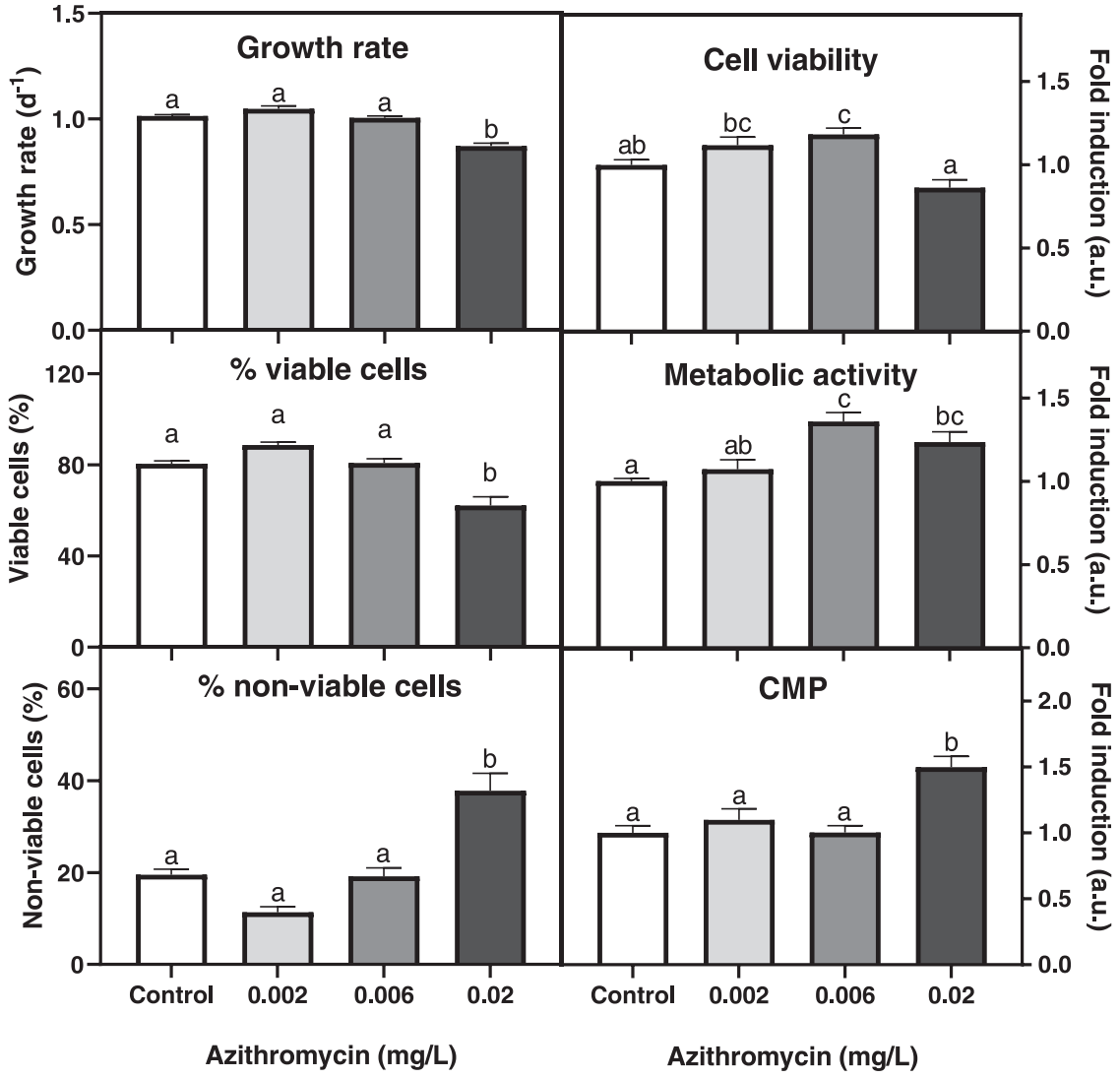

Fig. 1. Growth rate (d^{-1}), percentage of viable and non-viable cells (%), cell viability (a.u.- arbitrary units), metabolic activity (a.u.) and cytoplasmatic membrane potential (CMP; a.u.) in *Raphidocelis subcapitata* exposed to azithromycin. The data (mean ± SEM) represent 2 independent studies. Different letters indicate significant differences between concentrations ($p < 0.05$).

values for each time point in Table A1.

The obtained data (Fig. 1) showed that azithromycin only affected microalgal growth at the highest tested concentration of 0.02 mg/L, with a 15% decrease compared to control. No significant differences were obtained between the control and the first two concentrations of 0.002 mg/L and 0.006 mg/L.

The percentage of viable and non-viable cells (Fig. 1), inversely correlated, showed that only the highest tested concentration (0.02 mg/L) significantly affected the viability of microalgal cells (18% decrease). The percentage of viable cells presented a similar profile to the growth rate. At the lowest tested concentration (0.002 mg/L) there was a slight increment in cell viability (8% increment), but not significantly different from the control.

Cell viability and metabolic activity (Fig. 1) showed a similar tendency, with an increase at intermediate concentrations, followed by a decrease. For cell viability, the second tested concentration (0.006 mg/L) presented values significantly higher than control (18% increment). For metabolic activity, the two highest tested concentrations were significantly higher than control (36% increment for 0.006 mg/L and 24% increment for 0.02 mg/L).

Regarding the cytoplasmatic membrane potential (CMP; Fig. 1), only microalgal cells at the highest tested concentration (0.02 mg/L) presented significantly higher values than control, with a 50% increase.

3.2.2. Cell size, cell complexity and pigments content

Cell size (Fig. 2) decreased at the two highest tested concentrations compared to the control (5% and 6% decreases for 0.006 mg/L and 0.02 mg/L, respectively). For cell complexity, only at the second tested concentration (0.006 mg/L) significant differences from control were observed, with a 7% decrease.

Regarding the pigments content in *R. subcapitata* (Fig. 2), there was a concentration dependent increment in this endpoint, being the two highest tested concentrations significantly higher than the control (12% increment for 0.006 mg/L and 20% increment for 0.02 mg/L).

3.2.3. Reactive oxygen species (ROS), mitochondrial membrane potential (MMP) and lipid peroxidation (LPO)

For the endpoints related to the formation of ROS (H_2DFFDA and DHR 123), mitochondrial membrane potential (MMP) and LPO, significant differences from control were only observed for the H_2DFFDA probe and LPO. For these two endpoints, significant differences from the control were only obtained for microalgae exposed to the highest tested concentration (0.02 mg/L), with a 44% and 6% increase for ROS and LPO, respectively.(Fig. 3).

3.2.4. DNA content and cell cycle

The cell cycle phases, G1, S and G2, were discriminated in exposed microalgae (Fig. 4). For the G1 phase, only the microalgae exposed to the highest concentration (0.02 mg/L) showed significant differences from the control, with a 26% increase. At the S phase, although no significant differences from the control were obtained, the lowest (0.002 mg/L) and highest (0.02 mg/L) tested concentrations were different, being the latest significantly lower than the former (15% decrease). More differences were obtained for the last phase, G2, with a significant decrease from the control at the two highest tested concentrations (27% and 28% decrease for 0.006 mg/L and 0.02 mg/L, respectively).

3.2.5. PSII performance

Control samples measured after the 72 h exposure by the PAM fluorometry showed a maximal PS II quantum yield (F_v/F_m) of 0.73 ± 0.004. Therefore, as more than 70% of the absorbed light was applied in photosynthesis, the microalgae cells were maintained in a good physiological status under the used experimental conditions. The obtained data showed a clear distinction between the tested concentration for several of the PSII performance parameters (Figs. 5 and 6).

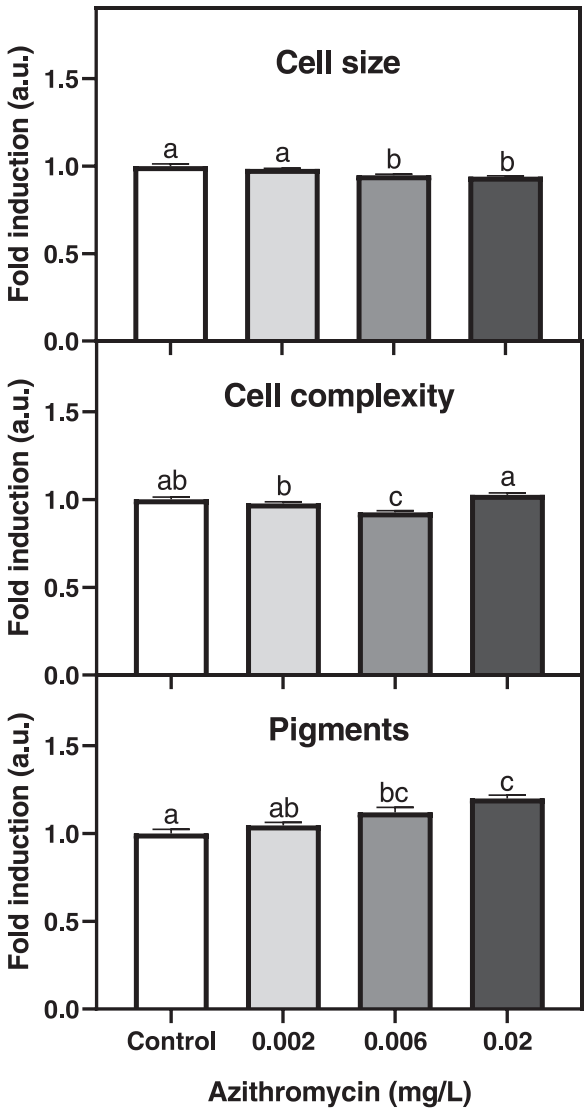

Fig. 2. Cell size, cell complexity and pigments content in *Raphidocelis subcapitata* exposed to azithromycin. All endpoints are expressed in arbitrary units (a.u.). The data (mean ± SEM) represent 2 independent studies. Different letters indicate significant differences between concentrations ($p < 0.05$).

F_v/F_m significantly decreased with increasing concentrations, up to a 24% decrease compared to the control for the highest tested concentration of 0.02 mg/L (Fig. 5). A similar trend was observed for the electron transport rate (ETR), showing a significant decrease up to 17% compared to the control. This endpoint also showed an increase of 3% for the lowest tested concentration (0.002 mg/L) compared to control. On the contrary, the efficiency of the oxygen-evolving complex (OEC) significantly increased at the two highest tested concentration, with a maximum of 118% increase compared to the control (0.02 mg/L).

The quantum yield parameters also showed significant differences between concentrations (Fig. 5). The effective PS II quantum yield (Y(II)), showed a similar pattern to that of ETR, with a significant decrease up to 17% for 0.02 mg/L. An exception was seen at 0.002 mg/L, where a small but significant increase of 3% was observed. The quantum yield of regulated energy dissipation (Y(NPQ)) showed a concentration-dependent decrease with a maximum of 47% decrease compared to the control (0.02 mg/L). This was opposite to the quantum yield of nonregulated energy dissipation (Y(NO)), where a significant concentration-dependent increase was seen, with a 49% maximum increase compared to control also at 0.02 mg/L.

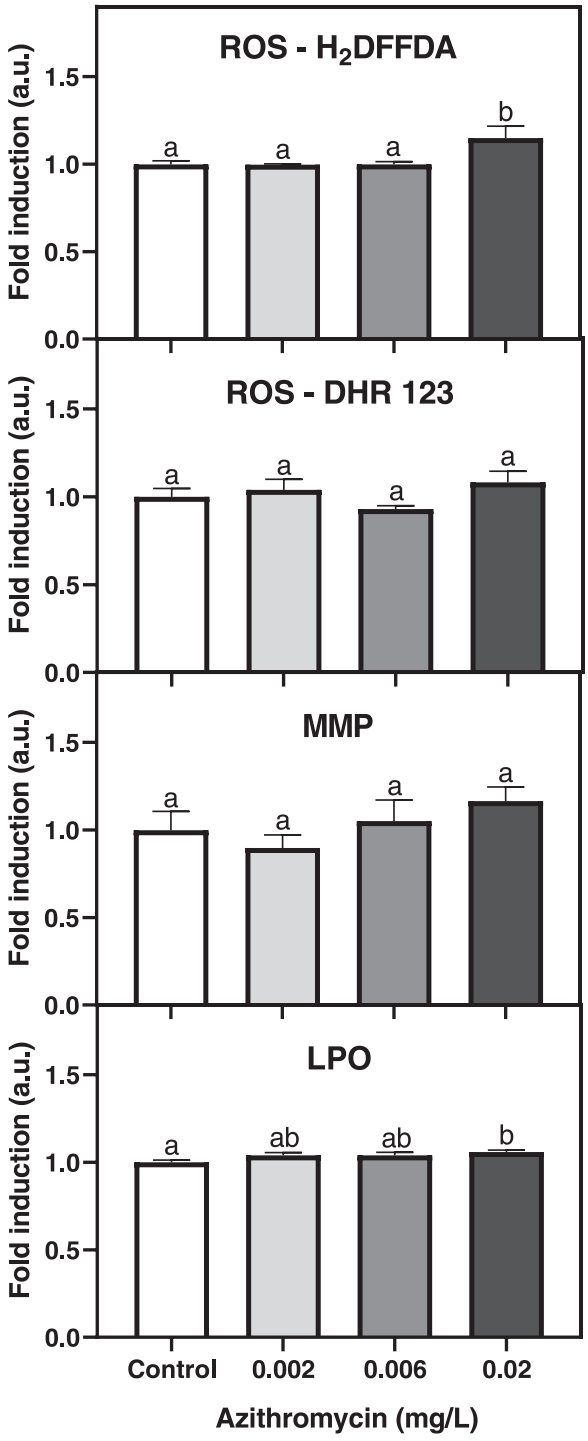

Fig. 3. Reactive oxygen species (ROS) formation measured as fluorescence of H_2DFFDA and DHR 123, mitochondrial membrane potential (MMP) and lipid peroxidation (LPO) in *Raphidocelis subcapitata* exposed to azithromycin. All endpoints are expressed in arbitrary units (a.u.). The data (mean ± SEM) represent 2 independent studies. Different letters indicate significant differences between concentrations ($p < 0.05$).

Similar alterations were observed for both photochemical quenching parameters, qP and qL, where a significant increase from the control was recorded at all tested concentrations (Fig. 6). A higher increment was observed for qL, up to 22% at 0.02 mg/L, compared to the control. On the other hand, both the coefficient of non-photochemical quenching (qN) and non-photochemical quenching (NPQ) significantly decreased with increasing concentrations, with the highest decrease being

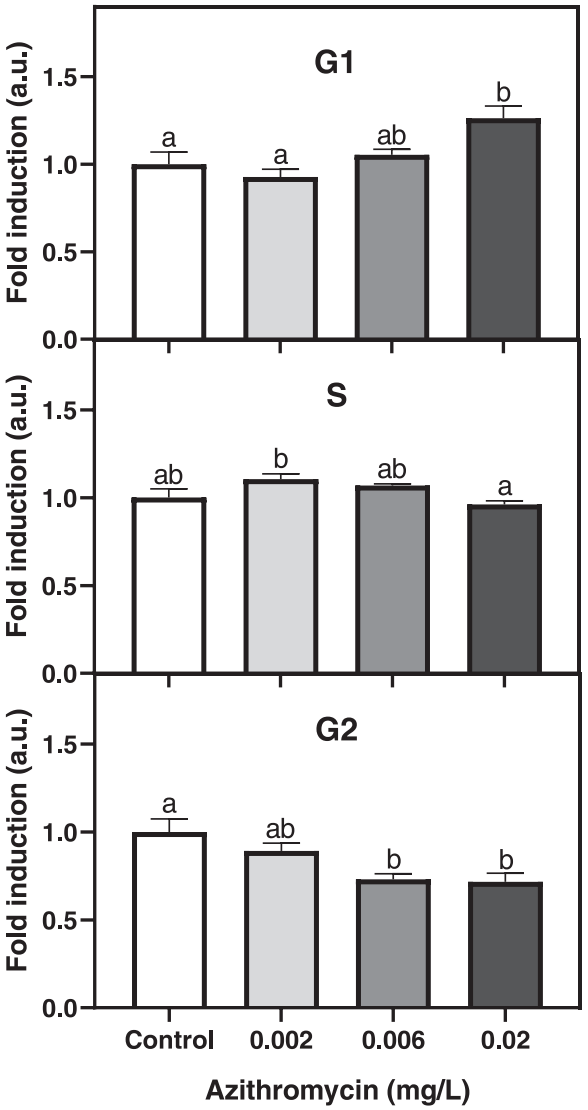

Fig. 4. DNA content indicated by PicoGreen in *Raphidocelis subcapitata* exposed to azithromycin. DNA content was used to differentiate three cell cycle phases, G1 (Gap phase), S (Synthesis – DNA replication), and G2 phases (growth). All endpoints are expressed in arbitrary units (a.u.). The data (mean ± SEM) represent 2 independent studies. Different letters indicate significant differences between concentrations ($p < 0.05$).

recorded for NPQ also at 0.02 mg/L (65% decrease compared to the control).

The relative distribution of the energy dissipation processes through photosystem II were different between the tested concentrations (Fig. 6). For the relative photochemical quenching ($qP_{(rel)}$), a concentration-dependent increase was recorded, with a maximum of 33% increase compared to the control for the highest concentration used (0.02 mg/L). The opposite was observed for the relative non-photochemical quenching ($qN_{(rel)}$), showing a concentration-dependent decrease, with the lowest value recorded for the highest tested concentration (42% decrease compared to the control). For the relative unquenched fluorescence ($UQF_{(rel)}$), a significant decrease from the control (12%) was only observed at the highest concentration.

3.3. Relation between endpoints

A PCA (Fig. 7; Table A5 in SI) was used to recognise patterns in the obtained data for azithromycin. The two axes explained 94% of the total

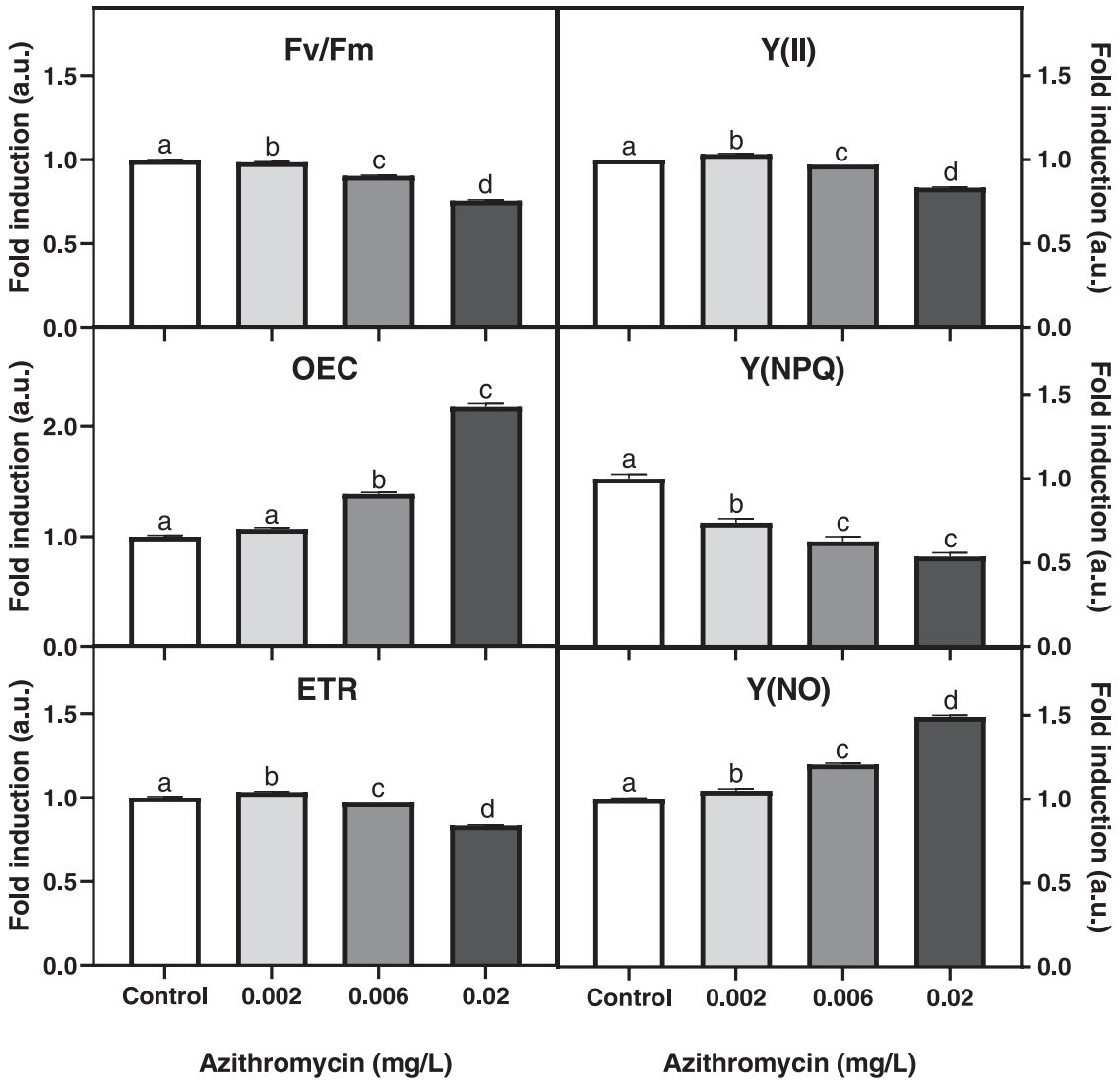

Fig. 5. PSII parameters of *Raphidocelis subcapitata* exposed to azithromycin. F_v/F_m – Maximal PSII quantum yield, OEC – Efficiency of oxygen-evolving complex, ETR – Relative photosynthetic electron transport rate, Y(II) - Effective PS II quantum yield, Y(NPQ) - Quantum yield of regulated energy dissipation, Y(NO) - Quantum yield of nonregulated energy dissipation. All endpoints are expressed in arbitrary units (a.u.). The data (mean ± SEM) represent 2 independent studies. Different letters indicate significant differences between concentrations ($p < 0.05$).

variance of data. PC1, accounting for 75% of data (eigenvalue 20.2), presented a clear discernment between the control together with the lowest concentration (0.002 mg/L) against the highest tested concentration (0.02 mg/L). The control and the lowest concentration were closely associated with the PSII performance endpoints Fv/Fm, $UQF_{(rel)}$, Y(II), ETR, NPQ, $qN_{(rel)}$, qN and Y(NPQ), growth rate, cell size and cell cycle phase G2. Contrariwise, the highest tested concentration was associated with the PSII performance endpoints Y(NO), qL, OEC, $qP_{(rel)}$ and qP, along with pigments content, cell cycle phase G1, ROS (carboxy-H_2DFFDA), cytoplasmatic and mitochondrial membrane potentials (CMP and MMP, respectively) and LPO.

To measure the correlation between all variables, a Pearson correlation analysis was used. The r^2 and *p*-values obtained are in Table A6 and A7, respectively, in the SI. Most of the correlations were observed between the PSII parameters, presenting the highest positive (Y(II) with ETR and qN with $qN_{(rel)}$) and negative correlations (Fv/Fm with Y(NO), NPQ with $qN_{(rel)}$). For the other biological endpoints, positive correlations were obtained between pigments with qL, Y(NO), qP, $qP_{(rel)}$ and OEC, and negative with Fv/Fm, NPQ, qN, $qN_{(rel)}$ and cell size. Growth rate showed a positive correlation with Y(II) and ETR, and negative with cell cycle phase G1, ROS and OEC. Cell cycle phase G1 had positive correlations with MMP, OEC and Y(NO) and negative with Y(II), ETR and Fv/Fm. On the other hand, cell cycle phase G2 showed positive correlations with cell size, qN, $qN_{(rel)}$, NPQ and Y(NPQ), and negative with qP(rel). The oxidative stress related endpoints (ROS, DHR 123, MMP and LPO) showed different correlations. ROS was positively correlated with CMP and OEC and negatively with growth rate, Y(II), ETR and $UQF_{(rel)}$. MMP only showed a positive correlation with cell cycle phase G1. LPO was positively correlated with qP and $qP_{(rel)}$ and negatively with NPQ, qN, $qN_{(rel)}$ and NPQ. Cell size had positive correlations with qN, $qN_{(rel)}$ and NPQ and negative with $qP_{(rel)}$. CMP showed only a negative correlation with $UQF_{(rel)}$. No correlations were obtained for the biological endpoints cell viability and complexity, metabolic activity, DHR 123 (ROS formation in mitochondria), and cell cycle phase S.

4. Discussion

Azithromycin, a broad-spectrum macrolide, is one of the most frequently administered antibiotics. Compared to erythromycin, which it is structurally related to, azithromycin is highly stable at low pH, having a long serum half-life and achieving higher concentrations in

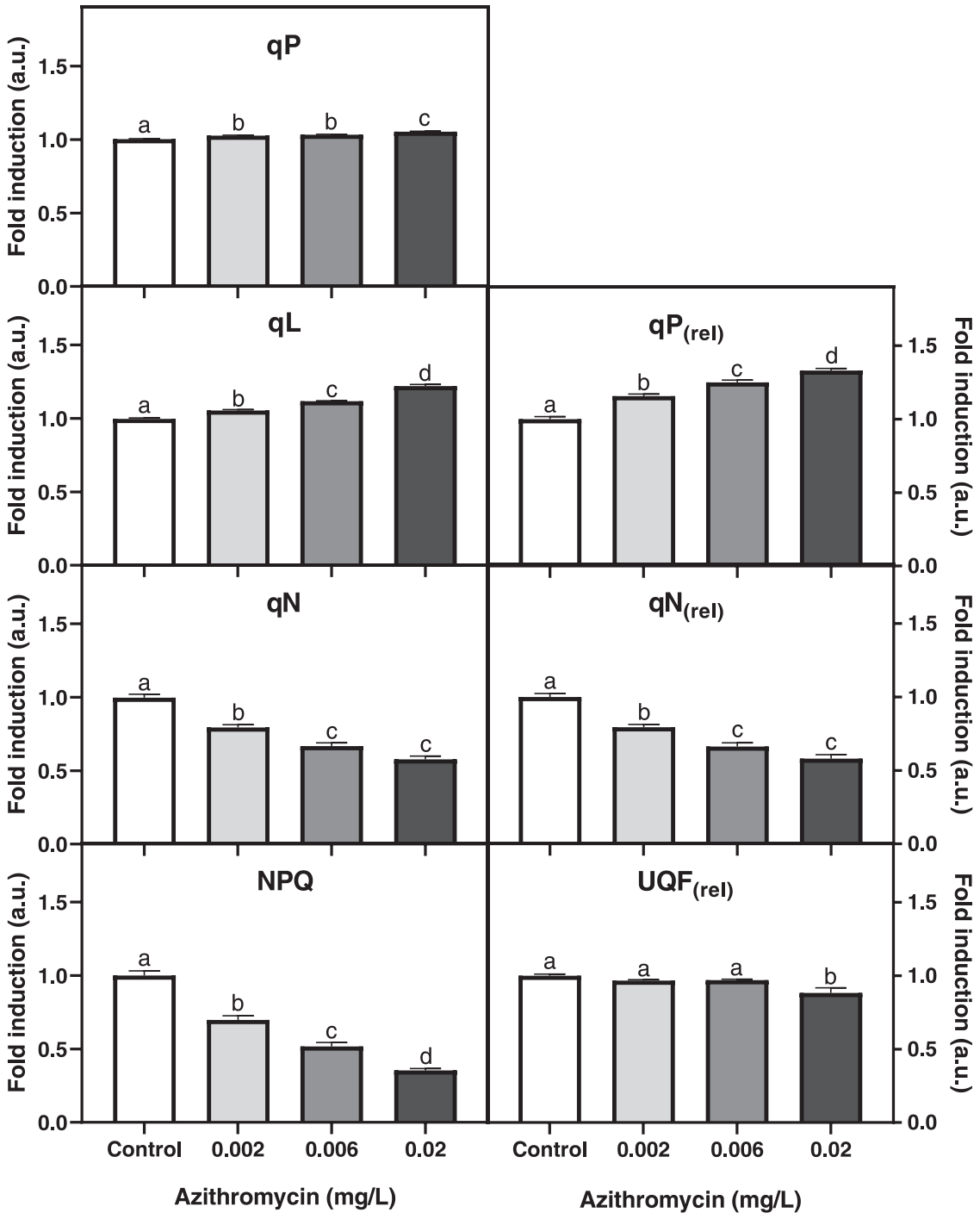

Fig. 6. Quenching parameters and distribution of dissipation energy processes through the PSII of *Raphidocelis subcapitata* exposed to azithromycin. qP and qL - Coefficients of photochemical quenching, qN - Coefficient of non-photochemical quenching, NPQ - Non-photochemical quenching, $qP_{(rel)}$ - Relative photochemical quenching, $qN_{(rel)}$ – Relative non-photochemical quenching, $UQF_{(rel)}$ – Relative unquenched fluorescence. All endpoints are expressed in arbitrary units (a.u.). The data (mean ± SEM) represent 2 independent studies. Different letters indicate significant differences between concentrations ($p < 0.05$).

tissues of biota. It is therefore considered as one of the most persistent antibiotics and of high environmental risk (Bielen et al., 2017; Fu et al., 2017). Although there are no regulations regarding surface water levels for any antibiotic, azithromycin is in the "watch list" within the European Water Framework Directive due to its toxicity, persistency and bioaccumulative potential (Aubakirova et al., 2017; Loos et al., 2018). Moreover, this antibiotic has also been included in the EU Watch List for EU monitoring concerning water policy by Commission Implementing Decision (EU) 2018/840 (EC, 2018).

Ecotoxicological risk assessment studies have already shown that this macrolide presents a risk to the aquatic environment (Alighardashi et al., 2014; Aubakirova et al., 2017; Välitalo et al., 2017; Zhou et al., 2016). Nevertheless, few studies have been conducted on the specific toxicity of azithromycin to microalgae, where only general toxicity endpoints such as effects on growth were analysed (Aubakirova et al., 2017; Fu et al., 2017; González-Pleiter et al., 2019, 2021; Kummerer and Henninger, 2003; Vestel et al., 2016; Zhou et al., 2016). In the present study, an EC_{50} of 0.051 mg/L for 72 h exposure was obtained. (Fu et al., 2017) reported an EC_{50} of 0.005 mg/L also for *R. subcapitata*, an order of magnitude lower than in the present study. Other studies reported $EC_{50\ s}$

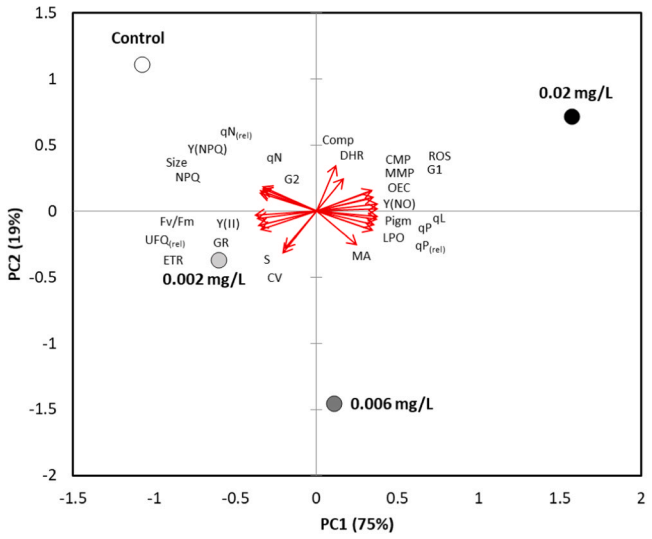

Fig. 7. Principal Component Analysis (PCA) of *Raphidocelis subcapitata* exposed to azithromycin. GR – Growth rate, Pigm – Pigments content: Chlorophyll *a* and *b*, carotenoids, xanthophyll, peridinin, ROS – Reactive oxygen species detected by carboxy-H_2DFFDA probe, DHR - Reactive oxygen species detected by DHR 123 probe, LPO – Lipid peroxidation, CV – Cell viability, MA – Metabolic activity, G1 – Gap phase in the cell cycle; S – Synthesis - DNA replication phase in the cell cycle, G2 – Growth phase in the cell cycle, Size – Cell size, Comp – Cell complexity, CMP - Cytoplasmatic membrane potential, MMP – Mitochondrial membrane potential, F_v/F_m – Maximum quantum yield, OEC – Efficiency of the oxygen-evolving complex, ETR – Electron transfer rate, Y(II) - Effective PS II quantum yield, Y(NPQ) - Quantum yield of regulated energy dissipation, Y(NO) - Quantum yield of nonregulated energy dissipation, qP and qL – Coefficients of photochemical quenching, qN – Coefficient of non-photochemical quenching, NPQ – Non-photochemical quenching, $qP_{(rel)}$ – Relative photochemical quenching, $qN_{(rel)}$ – Relative non-photochemical quenching, $UQF_{(rel)}$ – Relative unquenched fluorescence.

between 0.0018 mg/L for an unspecified blue-green alga (Vestel et al., 2016) to 0.33 mg/L for *Chlorella* sp. (Aubakirova et al., 2017). As these EC_{50} values are lower than 1 mg/L, this substance is classified as very toxic to the aquatic environment according to environmental classifications, labelling and packaging of substances and mixtures (EC, 2008, 2011).

At the lowest tested concentrations of 0.002 and 0.006 mg/L, a small increment in growth rate and cell viability was observed. It has already been observed in other studies that microalgae exposed to low doses of pharmaceuticals can show an increase in growth, suggesting the inductive effect hormesis (Miazek and Brozek-Pluska, 2019). (Zhang et al., 2019) detected a stimulation of *Chlorella pyrenoidosa* growth when exposed to low doses of lofibric acid, ciprofloxacin, diclofenac and carbamazepine. Low concentrations of sulphonamides (sulfacetamide and sulfamethoxazole) photodegradation products stimulated growth of *Chlorella vulgaris* (Baran et al., 2006). Florfenicol present at low concentrations also stimulated the growth of *Skeletonema costatum* (Liu et al., 2012). It has also been reported that some species can use pharmaceuticals as carbon sources. This is the case of *Chlorella* sp. using paracetamol, salicylic acid and diclofenac (Escapa et al., 2016, 2017), and *Phaeodactylum tricornutum* using bezafibrate (Duarte et al., 2019) as carbon sources.

The growth rate is however an integrative endpoint instigated by the interference with several subcellular processes. Therefore, by only analysing this general parameter, no information is obtained on its specific toxicity (i.e., MoA) to microalgae (Esperanza et al., 2015). It is already known that in bacteria, azithromycin inhibits protein synthesis by binding to the 23S rRNA of the bacterial 50 S ribosomal subunit. This binding step stops protein synthesis by inhibiting the transpeptidation/translocation step and assemblance of the 50 S ribosomal subunit. However, molecular studies suggest that the MoA of macrolides in bacteria and microalgae are different, as distinct pathways are targeted (Guo et al., 2020). To date, no studies were found investigating the specific toxic effects of azithromycin on microalgae. This study intended to complement the general knowledge on the toxicity of azithromycin to *R. subcapitata* with specialized biological endpoints. To accomplish this objective, a high-throughput methodology was set combining FCM (endpoints: pigments, cell size, complexity and viability, cell cycle, DNA content, ROS, CMP, MMP and LPO) with PAM fluorometry (PSII performance parameters).

In the present work, the photosynthetic capacity of *R. subcapitata* was clearly affected by azithromycin. The PCA showed that the majority of the PSII efficiency parameters along with pigments content were the most affected endpoints, explaining the toxicity of this antibiotic. This finding is in line with what has been seen in other studies, where other antibiotics have inhibited pathways in the chloroplasts of green algae (Bradel et al., 2000; Halling-Sørensen, 2000; Kasai et al., 2004; Liu et al., 2011b). As these are semi-autonomous organelles, antibiotics may interfere with photosynthesis by affecting protein synthesis, disturbing photosynthetic mechanisms and ultimately disturbing algal growth (Liu et al., 2011b), as observed in the present study. Nonetheless, as the tested concentrations were lower than the EC_{20} (EC_{20} =0.026 mg/L), a complete inhibition in photosynthetic processes was not observed in the exposed microalgae.

Y(NO), the quantum yield related with the regulated energy dissipation at PSII centers, increased in microalgae exposed to azithromycin. This shows that both photochemical energy conversion and protective regulatory machinery were not sufficient to protect the cells, with microalgae having difficulties in coping with radiation and becoming photodamaged (Kramer et al., 2004). The relative distribution of energy dissipation processes through the PSII exposed that the photochemical quenching was promoted to dissipate the existent excess of light energy. This was evident from the increase of both coefficients of photochemical quenching, qL and qP, as well as the decrease of the non-photochemical coefficients qN, $qN_{(rel)}$ and NPQ and the relative unquenched fluorescence $UQF_{(rel)}$. This dissipation process was however not enough to prevent damage. Interestingly, as previously seen by the authors (Almeida et al., 2019, 2017), the relative quenching parameters $qP_{(rel)}$ and $qN_{(rel)}$ better discriminated alterations in the photosynthetic and energy dissipation processes compared to qP and qN (Buschmann, 1995; Genty et al., 1989; Juneau et al., 2005).

The three quantum yields Fv/Fm, Y(NPQ) and Y(II) decreased in the exposed microalgae, confirming the impact of azithromycin in the photosynthetic capacity of PSII, which originated an overall decrease in photosynthetic performance. This has been observed in microalgae exposed to several contaminants (Kumar et al., 2014; Ralph et al., 2007), including to the antibiotic etruscomycin (Bishop, 1974), where a decrease/impairment in PSII parameters impacted the PSII photochemistry and electron transport chain in algae. The weakening of photosynthetic processes in *R. subcapitata* exposed to azithromycin was additionally confirmed by the increase in OEC and reduction in ETR, demonstrating the capacity of azithromycin to impact the electron transport chain. It has been previously shown that the antibiotics levofloxacin and amphotericin B significantly inhibited the photosynthetic electron transport in algae (Pan et al., 2009; Sandmann and Böger, 1981). Alterations in OEC, which reflects the state of the water photo-oxidation process, directly impact PSII photochemistry, originating a reduction in electron transfer between photosystems (Kriedemann et al., 1985). A reduction in ETR, the rate of electrons flow through the photosynthetic chain, will affect the PSII–PSI electron transport and all biochemical processes linked to photosynthesis. This will negatively affect all the photosynthetic processes and, consequently, the physiological state of microalgae (Juneau and Popovic, 1999).

In addition to alterations in PSII performance, an increase in natural pigments content (i.e., chlorophyll *a* and *b*, carotenoids, xanthophyll and

peridinin) was also detected in microalgae exposed to azithromycin. Chlorophyll *a* determined by FCM is related to the maximum fluorescence when the PSII reaction centers are locked in the Qy state. Accordingly, the inhibition of electron flow in the reaction centers located in the acceptor side of the PSII causes an increase in chlorophyll *a* fluorescence (Franqueira et al., 2000), as seen in exposed microalgae. An increase in chlorophyll *a* associated with the blockage of ETR at the PSII level has also been detected by (Seoane et al., 2014) in *Tetraselmis suecica* in response to the antibiotics chloramphenicol, florphenicol and oxytetracycline. The authors suggested that the increase in autofluorescence was indicative of an inhibition on PSII's oxidant side, possibly due to suppression of PS II reaction centres (Seoane et al., 2014). The close association between pigments content and PSII performance in *R. subcapitata* exposed to azithromycin was further confirmed by the correlation analysis. Negative correlations were obtained between pigments content and F_v/F_m, qN and NPQ, as well as positive correlations with Y(NO), OEC, qL and qP. In addition to a role in photosynthesis, some natural pigments have other accessorial functions to counteract the harmful effects of contaminants. This is the case of carotenoids, well-known antioxidant molecules important for scavenging ROS in microalgae. Carotenoids are not only involved in light collection, but also in the protection of the photosynthetic apparatus against ROS-associated damage (Knauert and Knauer, 2008). It has already been observed that in *R. subcapitata* exposed to low doses of the macrolide clarithromycin, carotenoids synthesis increased, allowing cells to increase their resistance towards this antibiotic (Peng et al., 2021).

The inhibition of photosynthetic performance, more precisely the reduction in ETR, can lead to oxidative stress due to the inhibition of release of excitation energy gathered by the PSII light harvesting complex (Hess, 2000). The relation between the impact of azithromycin in the photosynthetic capacity of *R. subcapitata*, the ROS formation and resulting oxidative stress was also emphasised in the PCA and correlation analysis. Significant correlations were detected between the PSII parameters and the oxidative stress endpoints, reinforcing the hypothesis that the PSII reaction centers may have suffered damage by ROS formation and/or vice-versa. It is well known that the PSI and PSII reaction centers in thylakoids are the main assembly locations of ROS in photosynthetic organisms (Almeida et al., 2017; Asada, 2006; Knauert and Knauer, 2008). Data obtained further indicated that ROS formed in chloroplasts was directly linked to an increase in OEC and decrease in ETR and $UFQ_{(rel)}$, leading to an overall decrease in the photosynthetic performance (Y(II)), and ultimately affecting growth. The formation of ROS in microalgal cells exposed to toxic agents (e.g. metals and pesticides) are known to originate damage to cellular membranes and cause a decrease in cell viability (e.g. (Prado et al., 2009). This seems to be consistent to what was observed in *R. subcapitata*, where a significant decrease in the % of viable cells and consequent decrease in cell viability was concomitant with an increase in CMP, evidencing damage to the integrity of microalgal membranes. Membrane hyperpolarization and alterations in membrane permeability were further evidenced by a rise in metabolic activity. This increase in FDA fluorescence is also indicative of a stimulus in esterase's activity, the enzymes vital for the renovation of phospholipids in membranes of cells (Franklin et al., 2001). Polyunsaturated fatty acids existing in phospholipids are susceptible to attack by ROS, whose damage can result in the disruption and collapse of cell membranes, and promote DNA fractionation (Halliwell and Gutteridge, 2015). Again, this was demonstrated by an increase in oxyradical formation responsible for LPO in *R. subcapitata*. In addition, significant correlations were observed between LPO and photosynthetic paraments related to photochemical and non-photochemical quenching, further evidencing the connection between energy dissipation in the PSII and oxidative damage. The cell cycle distribution of DNA content analysed using the fluorescence probe PicoGreen showed a potential reduction in cell division and/or genotoxic effects of azithromycin to microalgae. In fact, DNA values at the G1 phase increased with exposure to azithromycin, while the opposite was observed for the G2 phase. It has already been suggested that antibiotics can affect DNA replication in algae (Liu et al., 2011b). So, the increase observed in G1 seems to indicate that microalgae exposed to azithromycin suffered apoptosis related to fractional DNA content, while control cells had higher DNA integrity (Alberts, 2008). The inability of *R. subcapitata* to terminate cell division could originate the build-up of photosynthetic pigments or collapse in the regulation of cellular volume due to high ROS levels, which correlates to the results discussed above. The effects of azithromycin on DNA content in *R. subcapitata* was further demonstrated by the negative correlations obtained between cell cycle phase G1 (indicative of fractional DNA) with algal growth and the PSII parameters Y(II), Fv/Fm and ETR. The cell cycle phase G2, indicative of increased DNA integrity, was positively correlated with cell size and the PSII parameters Y(NPQ), qN and NPQ. These results demonstrated once more the importance of non-photochemical processes as the main dissipation of energy in exposed microalgae and are in line with what has been seen in other studies. Other macrolides such as clarithromycin, roxithromycin and erythromycin negatively affected not only the xenobiotic metabolism of exposed *R. subcapitata*, but also their electron transport and energy synthesis (Guo et al., 2020, Guo et. 2021; Peng et al., 2021). In a tentative for compensating the loss of energy, photosynthesis increased in exposed microalgae to obtain more energy. However, the over-excitation of light-collecting antenna and light intensity can also lead to an increment in ROS formation, instigating genotoxicity and DNA damage (Peng et al., 2021).

Finally, no alterations in ROS formation in the mitochondria and MMP were recorded in *R. subcapitata* in response to azithromycin, suggesting that azithromycin does not have an impact in these organelles.

5. Conclusions

The present study clearly identified the specific toxic effects of azithromycin to *R. subcapitata*. This macrolide inhibited pathways in photosynthesis by negatively impacting the regulation of energy dissipation at the PSII centers. The photochemical energy conversion and defensive controlling machinery in the exposed microalgae were insufficient, leading to difficulties to cope with radiation and promoting photodamage. The inefficient photochemical energy conversion, insufficient protective system and the possible blockage of the photosynthetic electron flow led to the formation of ROS and subsequent oxidative damage, affecting membranes and DNA integrity. Moreover, the methods described herein offer significant benefits to standardised regulatory accepted methods to improve hazard and risk assessment of contaminants in the environment and should be promoted for biological effects assessments in the future.

CRediT authorship contribution statement

Ana Catarina Almeida: Conceptualization, Methodology, Investigation, Formal analysis, Visualization, Writing – original draft, Project administration. **Tânia Gomes**: Methodology, Investigation, Formal analysis, Writing – original draft. **Jose Antonio Baz Lomba**: Methodology, Investigation, Formal analysis, Writing – original draft. **Adam Lillicrap**: Resources, Writing – review & editing, Funding acquisition, Project administration.

Declaration of Competing Interest

The authors declare that they have no known competing financial interests or personal relationships that could have appeared to influence the work reported in this paper.

Acknowledgments

This work was funded by the Norwegian Institute for Water Research

(NIVA) strategic research programme (Grant/contract number 160016).

Appendix A. Supporting information

Supplementary data associated with this article can be found in the online version at doi:10.1016/j.ecoenv.2021.112553.

References

Adler, N.E., Schmitt-Jansen, M., Altenburger, R., 2007. Flow cytometry as a tool to study phytotoxic modes of action. Environ. Toxicol. Chem. Int. J. 26, 297–306.

Alberts, B., 2008. Molecular Biology of the Cell. Garland Science.

Alighardashi, A., et al., 2014. Environmental risk assessment of selected antibiotics in Iran. Iran. J. Health Saf. Environ. 1, 132–137.

Almeida, A.C., Gomes, T., Langford, K., Thomas, K.V., Tollefsen, K.E., 2017. Oxidative stress in the algae Chlamydomonas reinhardtii exposed to biocides. Aquat. Toxicol. 189, 50–59.

Almeida, A.C., Gomes, T., Habuda-Stanić, M., Lomba, J., Romić, Ž., Turkalj, J.V., Lillicrap, A., 2019. Characterization of multiple biomarker responses using flow cytometry to improve environmental hazard assessment with the green microalgae Raphidocelis subcapitata. Sci. Total Environ. 687, 827–838.

Aristilde, L., Melis, A., Sposito, G., 2010. Inhibition of photosynthesis by a fluoroquinolone antibiotic. Environ. Sci. Technol. 44, 1444–1450.

Asada, K., 2006. Production and scavenging of reactive oxygen species in chloroplasts and their functions. Plant Physiol. 141, 391–396.

Aubakirova, B., et al., 2017. The effect of pharmaceutical ingredients to the growth of algae. БИОЛОГИЯ ЖӘНЕ МЕДИЦИНА СЕРИЯСЫ. 5 5 2017.

Baran, W., Sochacka, J., Wardas, W., 2006. Toxicity and biodegradability of sulfonamides and products of their photocatalytic degradation in aqueous solutions. Chemosphere 65, 1295–1299.

Bielen, A., Šimatović, A., Kosić-Vukšić, J., Senta, I., Ahel, M., Babić, S., Jurina, T., González Plaza, J.J., Milaković, M., Udiković-Kolić, N., 2017. Negative environmental impacts of antibiotic-contaminated effluents from pharmaceutical industries. Water Res. 126, 79–87.

Birošová, L., Mackulak, T., Bodík, I., Ryba, J., Škubák, J., Grabic, R., 2014. Pilot study of seasonal occurrence and distribution of antibiotics and drug resistant bacteria in wastewater treatment plants in Slovakia. Sci. Total Environ. 490, 440–444.

Bishop, D., 1974. The effect of polyene antibiotics on photosynthetic electron transfer. J. Exp. Bot. 25, 491–502.

Bradel, B.G., Preil, W., Jeske, H., 2000. Remission of the free-branching pattern of Euphorbia pulcherrima by tetracycline treatment. J. Phytopathol. 148, 587–590.

Buschmann, C., 1995. Variation of the quenching of chlorophyll fluorescence under different intensities of the actinic light in wildtype plants of tobacco and in an aurea mutant deficient of lightharvesting-complex. J. Plant Physiol. 145, 245–252.

Duarte, B., Prata, D., Matos, A.R., Cabrita, M.T., Caçador, I., Marques, J.C., Cabral, H.N., Reis-Santos, P., Fonseca, V.F., 2019. Ecotoxicity of the lipid-lowering drug bezafibrate on the bioenergetics and lipid metabolism of the diatom Phaeodactylum tricornutum. Sci. Total Environ. 650, 2085–2094.

Ebert, I., Bachmann, J., Kühnen, U., Küster, A., Kussatz, C., Maletzki, D., Schlüter, C., 2011. Toxicity of the fluoroquinolone antibiotics enrofloxacin and ciprofloxacin to photoautotrophic aquatic organisms. Environ. Toxicol. Chem. 30, 2786–2792.

EC, 2008. 1272/2008,'Regulation (EC) No 1272/2008 of the European Parliament and of the Council of 16 December 2008 on classification, labelling and packaging of substances and mixtures, amending and repealing Directives 67/548/EEC and 1999/45/EC, and amending Regulation (EC) No 1907/2006'. Official Journal of the European Union. 50, 353.

EC, 2011. Commission Regulation (EU) No 286/2011 of 10 March 2011 amending, for the purposes of its adaptation to technical and scientific progress, Regulation (EC) No 1272/2008 of the European Parliament and of the Council on classification, labelling and packaging of substances and mixtures Text with EEA relevance. Official Journal of the European Union L. 83.

EC, 2018. Comission Implementing Decision (EU) 2018/840 of 5 June 2018 establishing a watch list of substances for Union-wide monitoring in the field of water policy pursuant to Directive 2008/105/EC of the European Parliament and of the Council and repealing Commission Implementing Decision (EU) 2015/495. Official Journal of the European Union L. 141/9.

EEA, Pharmaceuticals in the Environment-Results of an EEA Workshop. EEA Copenhagen, Denmark, 2010.

Escapa, C., Coimbra, R.N., Paniagua, S., García, A.I., Otero, M., 2016. Comparative assessment of diclofenac removal from water by different microalgae strains. Algal Res. 18, 127–134.

Escapa, C., Coimbra, R.N., Paniagua, S., García, A.I., Otero, M., 2017. Paracetamol and salicylic acid removal from contaminated water by microalgae. J. Environ. Manag. 203, 799–806.

Esperanza, M., Cid, Á., Herrero, C., Rioboo, C., 2015. Acute effects of a prooxidant herbicide on the microalga Chlamydomonas reinhardtii: screening cytotoxicity and genotoxicity endpoints. Aquat. Toxicol. 165, 210–221.

Esperanza, M., Houde, M., Seoane, M., Cid, Á., Rioboo, C., 2017. Does a short-term exposure to atrazine provoke cellular senescence in Chlamydomonas reinhardtii? Aquat. Toxicol. 189, 184–193.

Franklin, N.M., Stauber, J.L., Lim, R.P., 2001. Development of flow cytometry-based algal bioassays for assessing toxicity of copper in natural waters. Environ. Toxicol. Chem. Int. J. 20, 160–170.

Franqueira, D., Orosa, M., Torres, E., Herrero, C., Cid, A., 2000. Potential use of flow cytometry in toxicity studies with microalgae. Sci. Total Environ. 247, 119–126.

Fu, L., Huang, T., Wang, S., Wang, X., Su, L., Li, C., Zhao, Y., 2017. Toxicity of 13 different antibiotics towards freshwater green algae Pseudokirchneriella subcapitata and their modes of action. Chemosphere 168, 217–222.

Gala, W.R., Giesy, J.P., 1990. Flow cytometric techniques to assess toxicity to algae. Aquatic Toxicology and Risk Assessment: Thirteenth Volume. ASTM International.

Genty, B., Briantais, J.M., Baker, N.R., 1989. The relationship between the quantum yield of photosynthetic electron transport and quenching of chlorophyll fluorescence. Biochim. Biophys. Acta BBA Gen. Subj. 990, 87–92.

Gomes, T., Almeida, A.C., Georgantzopoulou, A., 2020. Characterization of cell responses in Rhodomonas baltica exposed to PMMA nanoplastics. Sci. Total Environ. 726, 138547.

González-Pleiter, M., et al., 2019. Ecotoxicological assessment of antibiotics in freshwater using cyanobacteria. Cyanobacteria. Elsevier,, pp. 399–417.

González-Pleiter, M., Leganés, F., Fernández-Piñas, F., 2017. Intracellular free Ca2+ signals antibiotic exposure in cyanobacteria. RSC Adv. 7, 35385–35393.

González-Pleiter, M., Pedrouzo-Rodríguez, A., Verdú, I., Leganés, F., Marco, E., Rosal, R., Fernández-Piñas, F., 2021. Microplastics as vectors of the antibiotics azithromycin and clarithromycin: effects towards freshwater microalgae. Chemosphere 268, 128824.

Grégori, G., et al., 2003. A flow cytometric approach to assess phytoplankton respiration. Advanced Flow Cytometry: Applications in Biological Research. Springer, pp. 99–106.

Guo, J., Bai, Y., Chen, Z., Mo, J., Li, Q., Sun, H., Zhang, Q., 2020. Transcriptomic analysis suggests the inhibition of DNA damage repair in green alga Raphidocelis subcapitata exposed to roxithromycin. Ecotoxicol. Environ. Saf. 201, 110737.

Guo, J., Ma, Z., Peng, J., Mo, J., Li, Q., Guo, J., Yang, F., et al., 2021. Transcriptomic analysis of Raphidocelis subcapitata exposed to erythromycin: The role of DNA replication in hormesis and growth inhibition. Journal of Hazardous Materials 402 (123512).

Halling-Sørensen, B., 2000. Algal toxicity of antibacterial agents used in intensive farming. Chemosphere 40, 731–739.

Halliwell, B., Gutteridge, J.M., 2015. Free Radicals in Biology and Medicine. Oxford University Press, USA.

Hess, F.D., 2000. Light-dependent herbicides: an overview. Weed Sci. 48, 160–170.

ISO , 2012. ISO 8692. Water quality-fresh water algal growth inhibition test with unicellular green algae.

Juneau, P., Popovic, R., 1999. Evidence for the rapid phytotoxicity and environmental stress evaluation using the PAM fluorometric method: importance and future application. Ecotoxicology 8, 449–455.

Juneau, P., Green, B.R., Harrison, P.J., 2005. Simulation of Pulse-Amplitude-Modulated (PAM) fluorescence: limitations of some PAM-parameters in studying environmental stress effects. Photosynthetica 43, 75–83.

Kasai, K., Kanno, T., Endo, Y., Wakasa, K., Tozawa, Y., 2004. Guanosine tetra-and pentaphosphate synthase activity in chloroplasts of a higher plant: association with 70S ribosomes and inhibition by tetracycline. Nucleic Acids Res. 32, 5732–5741.

Kemper, N., 2008. Veterinary antibiotics in the aquatic and terrestrial environment. Ecol. Indic. 8, 1–13.

Knauert, S., Knauer, K., 2008. The role of reactive oxygen species in copper toxicity to two freshwater green algae 1. J. Phycol. 44, 311–319.

Kramer, D.M., Johnson, G., Kiirats, O., Edwards, G.E., 2004. New fluorescence parameters for the determination of QA redox state and excitation energy fluxes. Photosynth. Res. 79, 209–218.

Kriedemann, P., Graham, R., Wiskich, J., 1985. Photosynthetic dysfunction and in vivo changes in chlorophyll a fluorescence from manganese-deficient wheat leaves. Aust. J. Agric. Res. 36, 157–169.

Kumar, K.S., Dahms, H.U., Lee, J.S., Kim, H.C., Lee, W.C., Shin, K.H., 2014. Algal photosynthetic responses to toxic metals and herbicides assessed by chlorophyll a fluorescence. Ecotoxicol. Environ. Saf. 104, 51–71.

Kummerer, K., Henninger, A., 2003. Promoting resistance by the emission of antibiotics from hospitals and households into effluent. Clin. Microbiol Infect. 9, 1203–1214.

Liu, B., Liu, W., Nie, X., Guan, C., Yang, Y., Wang, Z., Liao, W., 2011a. Growth response and toxic effects of three antibiotics on Selenastrum capricornutum evaluated by photosynthetic rate and chlorophyll biosynthesis. J. Environ. Sci. 23, 1558–1563.

Liu, B., Nie, X., Liu, W., Snoeijs, P., Guan, C., Tsui, M.T.K., 2011b. Toxic effects of erythromycin, ciprofloxacin and sulfamethoxazole on photosynthetic apparatus in Selenastrum capricornutum. Ecotoxicol. Environ. Saf. 74, 1027–1035.

Liu, W., Ming, Y., Huang, Z., Li, P., 2012. Impacts of florfenicol on marine diatom Skeletonema costatum through photosynthesis inhibition and oxidative damages. Plant Physiol. Biochem. 60, 165–170.

Loos, R., et al., 2018. Review of the 1st Watch List Under the Water Framework Directive and Recommendations for the 2nd Watch List. Publications Office of the European Union., Luxembourg.

Marie, D., Vaulot, D., Partensky, F., 1996. Application of the novel nucleic acid dyes YOYO-1, YO-PRO-1, and PicoGreen for flow cytometric analysis of marine prokaryotes. Appl. Environ. Microbiol. 62, 1649–1655.

Martinez, R.S., Di Marzio, W.D., Sáenz, M.E., 2015. Genotoxic effects of commercial formulations of Chlorpyrifos and Tebuconazole on green algae. Ecotoxicology 24, 45–54.

Miazek, K., Brozek-Pluska, B., 2019. Effect of PHRs and PCPs on microalgal growth, metabolism and microalgae-based bioremediation processes: A Review. Int J. Mol. Sci. 20, 20.

Míguez, L., Esperanza, M., Seoane, M., Cid, Á., 2021. Assessment of cytotoxicity biomarkers on the microalga Chlamydomonas reinhardtii exposed to emerging and priority pollutants. Ecotoxicol. Environ. Saf. 208, 111646.

OECD , 2011. Test No. 201: Freshwater Alga and Cyanobacteria, Growth Inhibition Test.
Pan, X., Zhang, D., Chen, X., Mu, G., Li, L., Bao, A., 2009. Effects of levofloxacin hydrochlordie on photosystem II activity and heterogeneity of Synechocystis sp. Chemosphere 77, 413–418.
Peng, J., Guo, J., Lei, Y., Mo, J., Sun, H., Song, J., 2021. Integrative analyses of transcriptomics and metabolomics in Raphidocelis subcapitata treated with clarithromycin. Chemosphere 266, 128933.
Pinckney, J.L., Hagenbuch, I.M., Long, R.A., Lovell, C.R., 2013. Sublethal effects of the antibiotic tylosin on estuarine benthic microalgal communities. Mar. Pollut. Bull. 68, 8–12.
Prado, R., García, R., Rioboo, C., Herrero, C., Abalde, J., Cid, A., 2009. Comparison of the sensitivity of different toxicity test endpoints in a microalga exposed to the herbicide paraquat. Environ. Int. 35, 240–247.
Prado, R., Rioboo, C., Herrero, C., Cid, Á., 2012a. Screening acute cytotoxicity biomarkers using a microalga as test organism. Ecotoxicol. Environ. Saf. 86, 219–226.
Prado, R., Rioboo, C., Herrero, C., Suárez-Bregua, P., Cid, Á., 2012b. Flow cytometric analysis to evaluate physiological alterations in herbicide-exposed Chlamydomonas moewusii cells. Ecotoxicology 21, 409–420.
Ralph, P.J., Smith, R.A., Macinnis-Ng, C.M.O., Seery, C.R., 2007. Use of fluorescence-based ecotoxicological bioassays in monitoring toxicants and pollution in aquatic systems. Toxicol. Environ. Chem. 89, 589–607.
Rodriguez-Mozaz, S., Vaz-Moreira, I., Varela Della Giustina, S., Llorca, M., Barceló, D., Schubert, S., Berendonk, T.U., Michael-Kordatou, I., Fatta-Kassinos, D., Martinez, J. L., Elpers, C., Henriques, I., Jaeger, T., Schwartz, T., Paulshus, E., O'Sullivan, K., Pärnänen, K., Virta, M., Do, T.T., Walsh, F., Manaia, C.M., 2020. Antibiotic residues in final effluents of European wastewater treatment plants and their impact on the aquatic environment. Environ. Int. 140, 105733.
Rojíčková, R., Maršálek, B., 1999. Selection and sensitivity comparisons of algal species for toxicity testing. Chemosphere 38, 3329–3338.
Sandmann, G., Böger, P., 1981. Inhibition of photosynthetic electron transport by amphotericin B. Physiol. Plant. 51, 326–328.
Schreiber, U., Quayle, P., Schmidt, S., Escher, B.I., Mueller, J.F., 2007. Methodology and evaluation of a highly sensitive algae toxicity test based on multiwell chlorophyll fluorescence imaging. Biosens. Bioelectron. 22, 2554–2563.
Seoane, M., Rioboo, C., Herrero, C., Cid, Á., 2014. Toxicity induced by three antibiotics commonly used in aquaculture on the marine microalga Tetraselmis suecica (Kylin) Butch. Mar. Environ. Res. 101, 1–7.
Stauber, J.L., Franklin, N.M., Adams, M.S., 2002. Applications of flow cytometry to ecotoxicity testing using microalgae. Trends Biotechnol. 20, 141–143.
Suzuki, S., Yamaguchi, H., Nakajima, N., Kawachi, M., 2018. Raphidocelis subcapitata (= Pseudokirchneriella subcapitata) provides an insight into genome evolution and environmental adaptations in the Sphaeropleales. Sci. Rep. 8, 1–13.
Välitalo, P., Kruglova, A., Mikola, A., Vahala, R., 2017. Toxicological impacts of antibiotics on aquatic micro-organisms: a mini-review. Int. J. Hyg. Environ. Health 220, 558–569.
Veldhuis, M., Kraay, G., Timmermans, K., 2001. Cell death in phytoplankton: correlation between changes in membrane permeability, photosynthetic activity, pigmentation and growth. Eur. J. Phycol. 36, 167–177.
Vestel, J., Caldwell, D.J., Constantine, L., D'Aco, V.J., Davidson, T., Dolan, D.G., Millard, S.P., Murray-Smith, R., Parke, N.J., Ryan, J.J., Straub, J.O., Wilson, P., 2016. Use of acute and chronic ecotoxicity data in environmental risk assessment of pharmaceuticals. Environ. Toxicol. Chem. 35, 1201–1212.
Zhang, Y., Guo, J., Yao, T., Zhang, Y., Zhou, X., Chu, H., 2019. The influence of four pharmaceuticals on Chlorellapyrenoidosa culture. Sci. Rep. 9, 1624.
Zhou, H., Ying, T., Wang, X., Liu, J., 2016. Occurrence and preliminarily environmental risk assessment of selected pharmaceuticals in the urban rivers. Sci. Rep. 6, 34928.